ministerie van verkeer en waterstaat

koninklijk nederlands meteorologisch instituut

The performance of drag relations in the WAQUA storm surge model

J.R.N. Onvlee

Technical reports: TR-149
Technische rapporten; TR-149

De Bilt, 1993

De Bilt 1993

Publicationnumber: Technical reports =
Technische rapporten; TR 149

p.o. box 201
3730 AE De Bilt
Wilhelminalaan 10
tel.+31 30 206 911
telex 470 96

UDC: 551.466.33
551.509.322
551.556.8
(261.26)

ISSN: 0169-1708

ISBN: 90-369-2030-2

© KNMI, De Bilt. All rights reserved. No part of this publication may be reproduced or transmitted in any form or by any means, electronic or mechanical, including photcopying, recording, or any information storage and retrieval system, without permission in writing from the publisher.

The performance of drag relations in the WAQUA storm surge model

J. Onvlee

January 1993

Contents:

Abstract

In most storm surge models, a drag relation is applied which parametrizes the wind-induced surface stress in terms of wind velocity alone. In the WAQUA/CSM-16 model, used to predict water elevations along the Dutch North Sea coast, the wind stress was modelled until recently by the linear drag relation of Smith and Banke (1975). A number of alternatives to this relation have been suggested. For two of these, a piece-wise continuous function provided by the Tidal Waters Division of Rijkswaterstaat and a Charnock drag formulation, the performance within the WAQUA system has been evaluated and compared to that of the Smith and Banke function. Fore- and hindcast analyses were made for all three drag relations for several periods of various types of weather, including four recent storms. Both the Charnock and Rijkswaterstaat drag relations represent a significant improvement over the Smith and Banke drag coefficient, particularly in the prediction and reconstruction of powerful surges during storm conditions. The Charnock and Rijkswaterstaat functions yield similar results for all weather types, the Charnock coefficient on average resulting in a slightly better agreement with observed surge levels; the standard deviation of the model errors is significantly smaller for the Charnock function. On the basis of these observations it is recommended that the Charnock drag formulation be implemented in the operational WAQUA system in the near future.

1 Introduction

The accurate estimate of the momentum flux between air and sea is an important issue in the development of coupled atmosphere-wave models. One of the main areas of contention concerns the best manner by which to parametrizate the wind-induced surface stress in terms of the bulk properties of atmosphere and ocean. The surface stress τ is normally expressed in terms of the wind velocity $\vec{U}_{10}$ as:

$$\vec{\tau} = \rho_a C_d \mid \vec{U}_{10} \mid \vec{U}_{10} \tag{1}$$

where ρ_a is the density of air at sea level, and C_d is the drag coefficient, a bulk parameter depending upon atmospheric conditions and wave state. On the basis of standard mixing length theory, the wind in the turbulent layer above

the sea surface is usually assumed to have a logarithmic vertical profile:

$$U(z) = \frac{u_*}{\kappa} ln(\frac{z}{z_o}) \tag{2}$$

where $u_* = \sqrt{(\tau/\rho_a)}$ is the friction velocity and the integration constant z_o is called the roughness length. An alternative definition of the drag coefficient C_d is then given by $C_d = u_*^2/U_{10}^2$.

Until recently, it was conventionally assumed that the drag coefficient C_d was either a constant or weakly dependent on the surface wind field. In most observational efforts to derive the wind stress empirically, C_d was therefore expressed as a linear function of the windspeed:

$$C_d = a + b\, U_{10} \tag{3}$$

Many of these empirically derived linear drag relations are summarized in a review article by Geernaert (1990).

In recent years it has become increasingly clear that this simple representation of the surface stress is inadequate. In reality the drag coefficient appears to be a complex function of both atmospheric conditions and wave state. Several studies have indicated a strong inverse correlation of C_d with wave age (Donelan 1982,1990, Geernaert et al. 1987, Geernaert 1990, Maat et al. 1991, Nordeng 1991). Donelan (1990) showed the wind drag to be largest at short fetches, when the dominant waves are relatively steep and actively breaking. Blake (1991) found the drag coefficient to be a function of wave height. Geernaert (1990) summarizes observational evidence linking the wind drag to widely different factors such as the time dependence of the wave spectrum, the depth of the basin in which C_d is measured, the presence of slicks, and the passage of fronts.

Thus, the interaction between atmosphere and sea state, and the manner in which this interaction determines the surface wind stress, appears to be very complex. Much effort has been spent in the past few years to develop dynamically coupled models in which the surface stress is parametrized in a physically more realistic manner. Theories attempting to describe the wave-dependence of the surface stress have been formulated by e.g. Kitaigorodskii (1973), Janssen (1981, 1989) and Toba et al. (1990). Efforts are now being made to incorporate these ideas in coupled wave-storm surge models. Integrated surge models of this type have been described by Wolf et al. (1988)

and Mastenbroek et al. (1991). In spite of these developments, most operational storm surge models still employ only a rough parametrization of wind drag in terms of wind velocity alone.

2 The WAQUA storm surge model

At KNMI, the two-dimensional WAQUA/CSM-16 storm surge model is used on an operational basis to predict water elevations along the Dutch and British North Sea coasts. The model covers the whole of the Northwest-European continental shelf from 12° W to 13° E and 48° N to 62° N with a grid spacing of $\frac{1}{4}^o$ in the WE direction and $\frac{1}{6}^o$ in the NS direction; this corresponds to a bin size of approximately 16 km. Within WAQUA, the dynamics of tides and surges is described by the depth-averaged shallow-water equations, which are solved by an alternating direction implicit finite difference scheme on a staggered grid. The water levels on the open boundaries beyond the edge of the continental shelf are prescribed by ten tidal harmonic constituents. The wind and pressure fields required to determine the air-sea interaction are obtained from the LAM meteorological model and interpolated onto the WAQUA grid. For a detailed description of the WAQUA system, the reader is referred to De Vries (1991).

In the original version of the WAQUA model implemented at KNMI, the linear drag relation proposed by Smith and Banke (1975) was employed to estimate the wind stress: $10^3 C_d = 0.63 + 0.066 \mid \vec{U} \mid$ (Verboom et al. 1987). Operational experience revealed that this relation is inadequate when it comes to describing powerful surges during storm conditions. Verification of the model predictions showed that at high wind velocities the drag, and consequently the wind-induced set-up, is underestimated significantly (Bouws and De Vries 1991). In order to obtain more accurate water level predictions under conditions of strong wind, a re-appraisal of the wind stress parametrization was considered necessary.

The aim of the investigation described in this report is to compare the performance of the original Smith and Banke drag law within WAQUA with that of a number of alternative wind stress parametrizations. On the basis of this comparison a recommendation can be made as to which drag relation should be employed in the WAQUA system in the future.

3 Alternative drag formulations

Two alternative drag formulations will be considered here. The first one has been proposed by the Tidal Waters Division of Rijkswaterstaat. It is a piece-wise continuous function, henceforth called the RWS function, which assumes the drag coefficient to be constant for both very high and very low wind speeds, and linear in the region in between:

$$C_d = \begin{cases} 0.00144 & \text{for } U_{10} < 10.2 \text{ m/s} \\ -0.0006 + 0.0002U_{10} & \text{for } 10.2 < U_{10} < 15.9 \text{ m/s} \\ 0.00258 & \text{for } U_{10} > 15.9 \text{ m/s} \end{cases} \quad (4)$$

The idea behind this particular form is that the wind stress is principally determined by the roughness of the sea surface. For very low wind speeds, C_d is expected to be constant since the water surface is smooth; this is confirmed by observations (Large and Pond 1981, Hasselmann et al. 1988, Blake 1991). At high wind velocities, the near-linearity of C_d is believed to break down because of wave breaking and white-capping. Thus, the shape of the RWS function does admit of some physical justification.

The RWS function was expected to result in more accurate predictions of surge heights during storm conditions than the Smith and Banke formulation; since the RWS drag coefficient increases far steeper with wind velocity than the Smith and Banke relation for winds of intermediate strength, it is likely to have a less strong tendency to underestimate surges at high wind velocities. The RWS drag relation was implemented in the operational version of WAQUA in December 1991. At that time, only a brief comparison with its predecessor had been made; a more thorough evaluation of the two drag relations still remained to be done.

The second alternative to the Smith and Banke formula to be examined here is the one proposed by Charnock (1955). On the basis of dimensional arguments, Charnock assumed the roughness length, z_o, to be a function of friction velocity only. He proposed the following relation for z_o:

$$z_o = \beta u_*^2 / g \quad (5)$$

where the dimensionless Charnock coefficient β is taken to be constant. Assuming the conventional logarithmic vertical wind velocity profile, this ex-

pression for z_o results in an implicit, non-linear relationship between drag coefficient and wind speed.

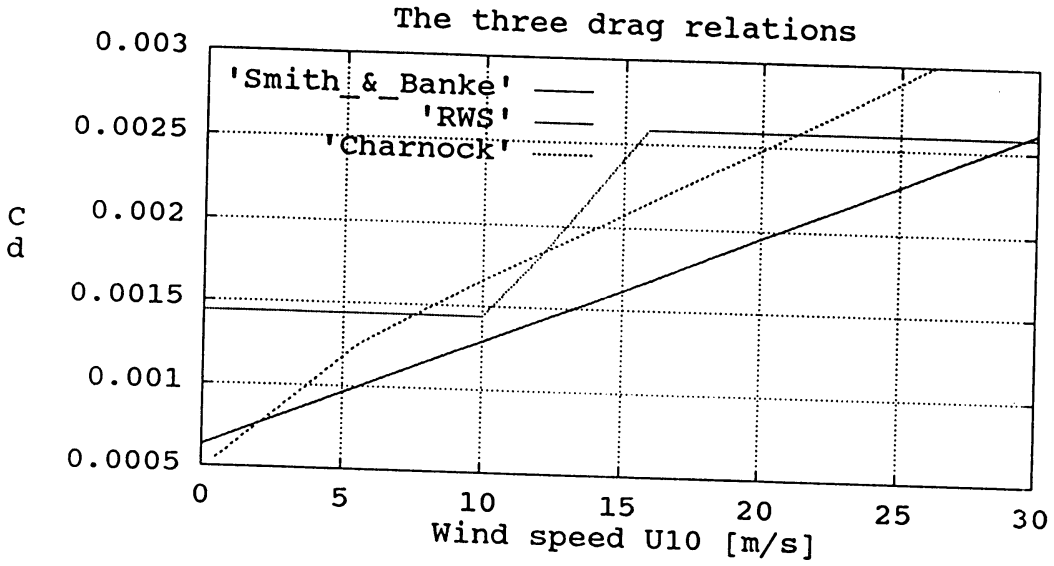

Figure 1: behaviour of the drag coefficient C_d as function of wind velocity U_{10} for various drag relations. The curve marked with '+' represents the Smith and Banke parametrization, crosses indicate the RWS function, and circles the Charnock drag coefficient for β=0.031.

The Charnock relation for z_o does not contain any direct reference to wave state parameters, implicitly assuming equilibrium between wind and the (high frequency) waves that primarily determine the roughness. As a consequence, the Charnock relation gives consistent results for fully developed seas, but is expected to be less appropriate for younger seas with growing wind waves (when the high frequency waves have a higher spectral level; Maat et al. 1991).

Experiments have yielded a wide range of values for the Charnock parameter β. Averaging over a wide range of circumstances, Wu (1980) found a mean β-value of 0.0185. A Charnock parameter of 0.0144 results in a drag

relation which is very similar to the one given by Smith and Banke.

In the following sections, we will examine the performance of the RWS and Charnock drag relations within the WAQUA system for a number of weather types, and compare this to the results obtained with the original Smith and Banke drag coefficient. All three drag formulations to be investigated are wave-independent and determined by the wind velocity alone. In view of the proven dependence of drag coefficient on wave state, a drag model in which the wind stress is coupled explicitly to wave properties would perhaps seem to be more appropriate than these relatively crude parametrizations. Several integrated wave-surge models have been constructed so far (Wolf et al. 1988, Mastenbroek et al. 1991), but although initial results for these models appear to be promising, further research remains to be done in this area. Secondly, whereas inserting a traditional wave-independent wind stress formulation in the operational WAQUA system is a straightforward thing to do, the implementation of a coupled wave-surge model would require considerably more effort. For the present investigation we will therefore limit ourselves to the three wave-independent drag relations described above.

4 The verification procedure

In order to assess the impact of the Smith and Banke, RWS and Charnock drag relations on the quality of the water level predictions made by WAQUA, fore- and hindcast analyses were made for all three drag relations for a number of periods. The time intervals selected for this investigation were chosen to be representative for the variety of weather conditions along the North Sea coast; they included a number of recent storms (February 1989, February 1990, December 1990 and December 1991), some periods of prolonged offshore wind (October 1990, January 1991) and several quieter intervals (April 1991, July 1991). The periods used in the analysis are listed in table 1. Observed values of water levels and high/low tides were provided by the Tidal Waters Division of Rijkswaterstaat.

At the time of this study, a test version of WAQUA was available including a Kalman filter (Voorrips and De Vries 1992). For the computations described below, the operational WAQUA system without Kalman filter was used.

In the case of the Charnock drag law, the free parameter β had to be tuned to average North Sea conditions first. Based on a large number of experiments covering a broad range of circumstances, Wu (1980) derived an average value of 0.0185 for β. For young seas and shallow, small basins such as the North Sea, β is expected to be larger than this mean value (Geernaert 1990). This indeed turns out to be the case. The best fit to the observed water elevations for all periods examined together is given by β=0.031 $\pm$ 0.002. Considering only the storm periods, the best fit to the observations is obtained by β=0.032 $\pm$ 0.001. Figure 1 shows the drag coefficient C_d as a function of wind velocity U_{10} for the Smith and Banke relation, the RWS function and the Charnock relation with β=0.031.

The results of the hindcast analyses for the three drag relations are presented in tables 2-4 and figs.2-17. Figures 2-11 show the surge (total - tidal) elevations at Hoek van Holland and Vlissingen for the negative surge of October 1990 and the storms of February 1989, February 1990, December 1990 and December 1991 for the Smith and Banke, RWS and Charnock drag relations. Figures 12-17 present scatter plots of the water levels predicted by the model, H_{mod}, as a function of observed elevations H_{obs} for a number of stations along the Dutch coast.

Tables 2-4 give statistical results of the verification of the three drag relations for the stations along the Dutch coast which are used by the Dutch Storm Tide Warning Service. The tables present the differences between calculated and observed skewed setup and times of the high and low tides, $H_{mod} - H_{obs}$ and $T_{mod} - T_{obs}$, together with their standard deviations. In addition to the statistics for all high and low tides, data are also shown for positive surges less than 0.80 m and negative surges less than 0.50 m. More extreme surges, positive or negative, are too rare for an analysis to be statistically meaningful.

5 Performance of the various drag relations

Inspection of the figures and tables shows that both the RWS and the Charnock drag relations represent a significant improvement over the Smith and Banke function originally implemented in WAQUA, particularly in the case of storm conditions. The powerful surges occurring in the storms that have been considered here are modelled far better by the two alternative

drag laws than by the Smith and Banke function, for which the surge heights are strongly underestimated (figs.2-11). This is also evident from the scatter plots (figs.12-17), in which the standard deviation of the cloud of data points from the diagonal is significantly less for the RWS and Chranock functions than for the Smith and Banke relation, especially in the regime of high surges.

For quiet summer periods with weak or intermediate-strength winds, all models were in good accordance with the observations. None of the three drag formulations is able to describe the negative surges caused by prolonged off-shore wind very well (e.g. figs.6,7); the smallest deviation from the observations is obtained with the Charnock drag representation. The implementation of a Kalman filter in the WAQUA model is likely to improve the predictive ability of the model at this point (Voorrips and de Vries, 1992).

During storm conditions, the RWS and Charnock drag coefficients yield comparable results. For the storm of February 1990, the RWS function gives the smallest discrepancies between model and observations, for the storms of February 1989, December 1990 and December 1991 the Charnock relation gives the best results. Summing all periods, the difference between calculated and observed elevations $< dH >$ for the Charnock function for most coastal stations is typically 0.5-1 cm less than for the RWS function (tables 3,4); additionally, the standard deviation of the model error $< dH >$ is significantly less for the Charnock relation than for the RWS drag coefficient.

One thing which should be kept in mind is that the potential accuracy of any drag relation is limited primarily by the quality of the meteorological data. Poor input wind and pressure fields will diminish the reliability of predicted water levels, and may distort our view of the performance of the drag relation applied. A good example of this is presented by the storm in December 1991, for which the LAM atmospheric model yielded forecasted and, to a lesser extent, analyzed wind fields which were much stronger than was actually observed (van Moerkerken 1992). Operationally predicted surge levels for most coastal stations were more than 50 cm too high. This large overestimate is probably largely due to the inaccuracy of the input wind fields, rather than to the drag coefficient applied (*in casu* the RWS function installed a few weeks earlier).

6 Conclusions

Both the RWS and Charnock drag relations represent a significant improvement over the Smith and Banke function by which the wind-induced set-up in WAQUA was originally modelled. In retrospect, the transition from the Smith and Banke drag law to the RWS relation in December 1991 is justified. The relatively large overestimate of the predicted water levels during the storm following this transition presumably was largely due to poor meteorological data.

When comparing the empirically derived RWS drag relation to the Charnock formulation, based on physical assumptions, the Charnock drag representation on average yields the closest agreement between observed and calculated water elevations. The differences between the surge levels predicted by the two drag relations are small, in the order of 1-2 centimeters; the standard deviation of the model error σ_H, however, is significantly less for the Charnock drag coefficient. During storm conditions, the Charnock relation on the whole is able to model powerful surges, both positive and negative, as well as or better than the RWS function. In view of these results, it is recommended that, pending the development of physically more realistic wave-dependent drag models, the Charnock drag formulation replace the RWS function in the operational WAQUA system.

Acknowledgements: The author wishes to thank Hans de Vries and Kees Mastenbroek for helpful comments and suggestions, Aart Voorrips for his assistance in the preparation of the report, and Hans de Vries and Leo Hafkenscheid for a critical reading of the paper. The work described in this report was performed in the context of, and funded by, the EC MAST project MAST-0050-C (PROFILE).

References:

Blake, R.A., 1991: "The dependence of wind stress on wave height and wind speed", *J. Geoph. Res.* **96 (C11)**, pp.20531-20545

Charnock, H., 1955: "Wind stress on a Water Surface", *Quart. J. Roy. Meteorol. Soc.* **81**, pp.639-640.

Donelan, M.A., 1982: "The dependence of the aerodynamic drag coefficient

on wave parameters", in *Proceedings of the First International Conference on Meteorology and air/sea interaction of the coastal zone*, Am. Meteor. Soc., Boston, Mass., pp.381-387

Donelan, M.A., 1990: "Air-sea interaction", *The Sea: Ideas and observations on progress in the study of the seas, Vol.9A, B. LeMehaute and D. Hanes (eds.)*, Wiley-Interscience, New York, pp.239-292.

Geernaert, G.L., Larsen, S.E., and Hansen, F., 1987: "Measurements of the wind stress, heat flux and turbulence intensity during storm conditions over the North Sea", *J. Geophys. Res.* **92(C5)**, pp.13127-13139

Geernaert, G.L., 1990: "Bulk parametrisations for the wind stress and heat fluxes", in *Surface Waves and Fluxes, Volume 1, G.L. Geernaert and W.J. Plant (eds.)*, Kluwer Academic Publishers, Dordrecht, pp.91-172.

Hasselmann, S., et al. (WAMDI group), 1988: "The WAM model - A third generation ocean wave prediction model", *J. Phys. Ocean.* **18**, pp.1775-1810

Janssen, P.A.E.M., 1981: "Quasi-linear approximation for the spectrum of wind-generated water waves", *J. Fluid Mech* **117**, pp.493-506

Janssen, P.A.E.M., 1989: "Wave-induced stress and the drag of air flow over sea waves", *J. Phys. Ocean.* **19**, pp.745-754.

Kitaigorodskii, S.A., 1973: "The physics of air-sea interaction", translated from Russian by Baruch, J., Israel Program for Scientific Translations, Jerusalem

Large, W., and Pond, S., 1981: "Open ocean momentum flux measurements in moderate to strong winds", *J. Phys. Ocean.* **11**, pp.324-336

Maat, N., Kraan., C., and Oost, W.A., 1991: "The roughness of wind waves", *Boundary-layer Meteorol.* **54**, pp.89-103.

Mastenbroek, C., Burgers, G., and Janssen, P.A.E.M., 1992: "The dynamical coupling of a wave model and a storm surge model through the atmospheric boundary layer", *submitted to J. Phys. Ocean.*

Moerkerken, R.A. van, 1992: *Monthly Bulletin North Sea, December 1991*

Nordeng, T.E., 1991: "On the wave age dependent drag coefficient and roughness length at sea", *J. Geoph. Res.* **96(C4)**, pp.7167-7174

Smith, S.D., and Banke, E.G., 1975: "Variation of the sea surface drag coefficient with wind speed", *Quart. J. Roy. Meteorol. Soc.* **101**, pp.665-673.

Verboom, G., Dijk, R. van, and Ronde, J. de, 1987: "Een model van het Europese Kontinentale plat voor windopzet en waterkwaliteitsbere-

keningen", Rijkswaterstaat-DGW, Waterloopkundig Laboratorium, GWAO 87.021, The Hague

Voorrips, A.C., Vries, J.W. de, 1992: "Real-time assimilation of sealevel data in the storm surge model WAQUA", KNMI memorandum OO-92-07, unpublished manuscript

Vries, J.W. de, 1991: "The implementation of the WAQUA/CSM-16 model for real-time storm surge forecasting", *Technical Report* TR-131, KNMI, De Bilt

Wu, J., 1980: "Wind stress coefficients over sea surface near neutral conditions. A revisit", *J. Phys. Ocean.* **10**, pp.727-740

Table 2: Hindcast analyses using a Smith and Banke drag relation

All tides:

Station	High tides						Low tides					
	$< dH >$ [m]	σH [m]	n	$< dT >$ [h]	σT [h]	n	$< dH >$ [m]	σH [m]	n	$< dT >$ [h]	σT [h]	n
Vlissingen	-0.02	0.16	151	-0.03	0.17	151	0.03	0.16	156	-0.11	0.22	156
Hoek van Holland	-0.02	0.14	150	-0.09	0.29	150	0.06	0.15	147	0.21	1.50	147
Ijmuiden	-0.04	0.17	144	0.04	0.31	144	0.03	0.13	134	-0.01	0.50	134
Den Helder	0.02	0.16	153	0.08	1.17	153	0.04	0.14	151	-0.00	0.31	151
Harlingen	0.05	0.20	140	-0.10	0.28	140	0.09	0.20	143	-0.11	0.24	143
West Terschelling	0.08	0.20	135	0.61	0.35	135	0.16	0.13	117	0.04	0.43	117
Huibertgat	0.00	0.18	144	-0.17	0.41	144	0.08	0.15	150	-0.23	0.42	150
Delfzijl	0.04	0.19	150	-0.13	0.31	150	0.08	0.21	150	-0.19	0.23	150

Positive surges less than 0.8m:

Station	High tides						Low tides					
	$< dH >$ [m]	σH [m]	n	$< dT >$ [h]	σT [h]	n	$< dH >$ [m]	σH [m]	n	$< dT >$ [h]	σT [h]	n
Vlissingen	-0.06	0.15	51	-0.05	0.16	51	-0.04	0.16	49	-0.10	0.27	49
Hoek van Holland	-0.07	0.12	57	-0.19	0.27	57	-0.04	0.11	44	0.07	1.66	44
Ijmuiden	-0.07	0.11	58	0.00	0.32	58	-0.05	0.12	50	0.05	0.59	50
Den Helder	-0.04	0.14	54	0.09	1.28	54	-0.05	0.11	64	-0.00	0.27	64
Harlingen	-0.03	0.17	51	-0.13	0.26	51	-0.03	0.13	52	-0.14	0.23	52
West Terschelling	-0.02	0.14	45	0.52	0.38	45	0.06	0.17	20	-0.15	0.72	20
Huibertgat	-0.04	0.16	54	-0.23	0.49	54	-0.05	0.12	59	-0.19	0.38	59
Delfzijl	-0.04	0.15	48	-0.19	0.27	48	-0.09	0.14	46	-0.29	0.20	46

Negative surges less than 0.5m:

Station	High tides						Low tides					
	$< dH >$ [m]	σH [m]	n	$< dT >$ [h]	σT [h]	n	$< dH >$ [m]	σH [m]	n	$< dT >$ [h]	σT [h]	n
Vlissingen	0.02	0.12	88	-0.01	0.18	88	0.07	0.11	95	-0.11	0.16	95
Hoek van Holland	0.04	0.10	87	-0.02	0.28	87	0.08	0.13	92	0.26	1.43	92
Ijmuiden	0.00	0.11	76	0.07	0.28	76	0.04	0.11	76	-0.05	0.43	76
Den Helder	0.06	0.10	90	0.07	1.12	90	0.05	0.09	72	-0.02	0.25	72
Harlingen	0.09	0.11	71	-0.08	0.27	71	0.17	0.13	77	-0.11	0.21	77
West Terschelling	0.03	0.11	69	0.66	0.29	69	0.20	0.15	87	0.09	0.32	87
Huibertgat	0.05	0.10	74	-0.11	0.23	74	0.10	0.12	79	-0.20	0.34	79
Delfzijl	0.05	0.12	80	-0.14	0.30	80	0.18	0.13	85	-0.13	0.20	85

Table 3: Hindcast analyses using an RWS drag relation

All tides:

Station	High tides						Low tides					
	$< dH >$ [m]	σH [m]	n	$< dT >$ [h]	σT [h]	n	$< dH >$ [m]	σH [m]	n	$< dT >$ [h]	σT [h]	n
Vlissingen	0.02	0.13	149	-0.03	0.20	149	0.05	0.13	155	-0.13	0.28	155
Hoek van Holland	0.02	0.11	149	0.00	0.37	149	0.05	0.13	147	-0.03	1.62	147
Ijmuiden	0.00	0.13	144	0.05	0.63	144	0.01	0.12	134	-0.03	0.61	134
Den Helder	0.01	0.13	153	-0.07	1.21	153	0.02	0.14	151	-0.01	0.37	151
Harlingen	0.06	0.18	140	-0.19	0.39	140	0.09	0.17	143	-0.09	0.28	143
West Terschelling	0.06	0.18	135	0.62	0.36	125	0.21	0.14	116	0.12	0.27	116
Huibertgat	0.04	0.14	144	-0.10	0.35	144	0.06	0.14	150	-0.11	0.29	150
Delfzijl	0.03	0.16	150	-0.12	0.33	150	0.04	0.23	150	-0.20	0.26	150

Positive surges less than 0.8m:

Station	High tides						Low tides					
	$< dH >$ [m]	σH [m]	n	$< dT >$ [h]	σT [h]	n	$< dH >$ [m]	σH [m]	n	$< dT >$ [h]	σT [h]	n
Vlissingen	-0.04	0.14	51	-0.05	0.21	51	0.04	0.18	49	-0.08	0.29	49
Hoek van Holland	-0.05	0.11	57	-0.08	0.42	57	0.03	0.14	44	-0.25	1.93	44
Ijmuiden	-0.04	0.13	58	-0.02	0.49	58	-0.02	0.12	50	0.02	0.68	50
Den Helder	-0.02	0.12	54	-0.05	1.28	54	-0.03	0.12	64	-0.04	0.30	64
Harlingen	0.02	0.17	51	-0.25	0.38	51	0.01	0.13	52	-0.15	0.28	52
West Terschelling	0.04	0.11	45	0.54	0.35	45	0.19	0.17	20	0.13	0.26	20
Huibertgat	0.02	0.11	54	-0.14	0.32	54	-0.01	0.13	59	-0.08	0.29	59
Delfzijl	0.02	0.13	48	-0.18	0.30	48	-0.06	0.13	46	-0.25	0.21	46

Negative surges less than 0.5m:

Station	High tides						Low tides					
	$< dH >$ [m]	σH [m]	n	$< dT >$ [h]	σT [h]	n	$< dH >$ [m]	σH [m]	n	$< dT >$ [h]	σT [h]	n
Vlissingen	0.02	0.09	89	-0.01	0.20	89	0.05	0.09	94	-0.12	0.19	94
Hoek van Holland	0.02	0.09	86	0.03	0.32	86	0.05	0.11	92	0.05	1.42	92
Ijmuiden	0.01	0.11	76	0.03	0.64	76	0.01	0.10	76	-0.04	0.49	76
Den Helder	0.05	0.08	90	-0.02	1.12	90	0.06	0.09	72	-0.05	0.30	72
Harlingen	0.08	0.09	71	-0.10	0.32	71	0.16	0.11	77	-0.09	0.22	77
West Terschelling	0.03	0.09	69	0.67	0.32	69	0.19	0.12	87	0.14	0.27	87
Huibertgat	0.04	0.10	74	-0.12	0.31	74	0.11	0.10	79	-0.15	0.22	79
Delfzijl	0.05	0.10	80	-0.13	0.34	80	0.15	0.10	85	-0.13	0.23	85

Table 4: Hindcast analyses using a Charnock drag relation(β=0.031)

All tides:

Station	High tides						Low tides					
	$< dH >$ [m]	σH [m]	n	$< dT >$ [h]	σT [h]	n	$< dH >$ [m]	σH [m]	n	$< dT >$ [h]	σT [h]	n
Vlissingen	0.00	0.11	149	-0.04	0.21	149	0.04	0.13	155	-0.13	0.26	155
Hoek van Holland	-0.02	0.10	149	-0.02	0.34	149	0.02	0.11	146	0.12	1.71	146
Ijmuiden	0.00	0.11	144	0.01	0.60	144	0.00	0.10	132	0.00	0.59	132
Den Helder	-0.02	0.11	153	-0.06	1.19	153	0.00	0.11	148	0.00	0.37	148
Harlingen	0.04	0.14	140	-0.18	0.38	140	0.07	0.13	143	-0.10	0.28	143
West Terschelling	0.04	0.10	135	0.61	0.37	135	0.17	0.12	116	0.11	0.26	116
Huibertgat	0.02	0.12	144	-0.11	0.36	144	0.04	0.13	148	-0.11	0.31	148
Delfzijl	0.01	0.14	150	-0.13	0.34	150	0.03	0.24	149	-0.23	0.26	149

Positive surges less than 0.8m:

Station	High tides						Low tides					
	$< dH >$ [m]	σH [m]	n	$< dT >$ [h]	σT [h]	n	$< dH >$ [m]	σH [m]	n	$< dT >$ [h]	σT [h]	n
Vlissingen	-0.03	0.13	51	-0.06	0.21	51	0.03	0.14	49	-0.09	0.29	49
Hoek van Holland	-0.03	0.10	57	-0.08	0.35	57	0.02	0.11	42	-0.04	2.15	42
Ijmuiden	-0.04	0.10	58	-0.03	0.47	58	-0.02	0.10	50	0.04	0.67	50
Den Helder	-0.03	0.10	54	-0.01	1.30	54	-0.02	0.08	64	-0.03	0.27	64
Harlingen	0.01	0.17	51	-0.22	0.37	51	0.01	0.10	52	-0.14	0.24	52
West Terschelling	0.04	0.09	45	0.53	0.32	45	0.17	0.12	19	0.12	0.27	19
Huibertgat	0.01	0.10	54	-0.15	0.33	54	-0.01	0.10	59	-0.07	0.34	59
Delfzijl	0.01	0.12	48	-0.22	0.31	48	-0.06	0.09	46	-0.28	0.20	46

Negative surges less than 0.5m:

Station	High tides						Low tides					
	$< dH >$ [m]	σH [m]	n	$< dT >$ [h]	σT [h]	n	$< dH >$ [m]	σH [m]	n	$< dT >$ [h]	σT [h]	n
Vlissingen	0.00	0.09	89	0.00	0.20	89	0.04	0.09	94	-0.12	0.18	94
Hoek van Holland	0.01	0.08	86	0.02	0.30	86	0.04	0.09	92	0.19	1.46	92
Ijmuiden	0.00	0.11	76	0.00	0.64	76	0.01	0.08	76	-0.03	0.50	76
Den Helder	0.04	0.07	90	-0.03	1.09	90	0.05	0.09	72	-0.05	0.30	72
Harlingen	0.07	0.07	71	-0.15	0.32	71	0.13	0.10	77	-0.09	0.21	77
West Terschelling	0.02	0.08	68	0.67	0.30	68	0.16	0.10	86	0.11	0.27	86
Huibertgat	0.02	0.10	74	-0.13	0.33	74	0.07	0.09	79	-0.13	0.23	79
Delfzijl	0.05	0.08	79	-0.12	0.35	79	0.12	0.11	85	-0.16	0.24	85

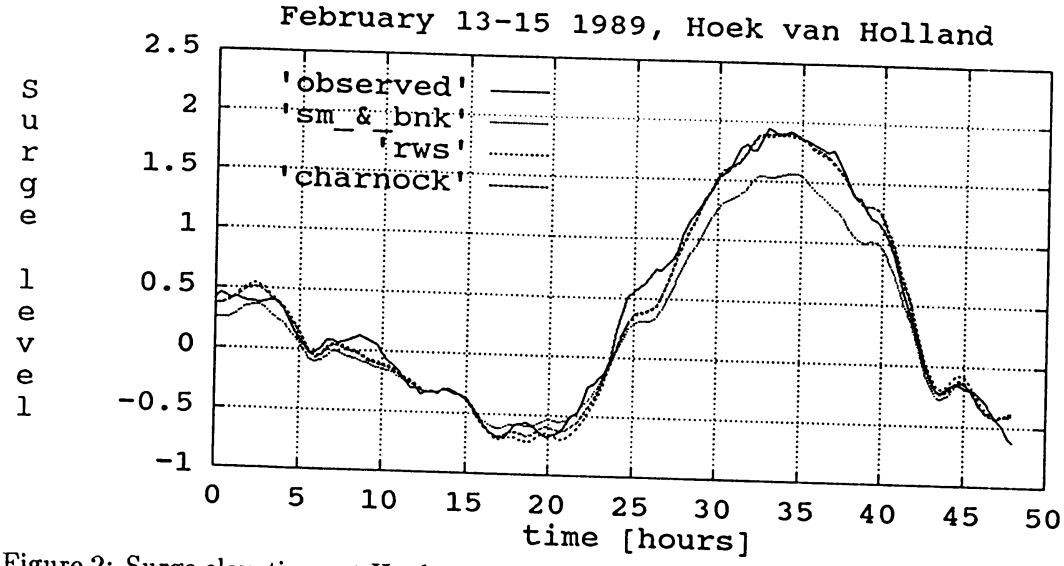

Figure 2: Surge elevations at Hoek van Holland for the February 1989 storm for the three drag models. The continuous curve represents the observations, the dotted curve the Smith and Banke drag relation, the thin-dashed curve the RWS function, and the thick-dashed curve the Charnock function for β=0.031.

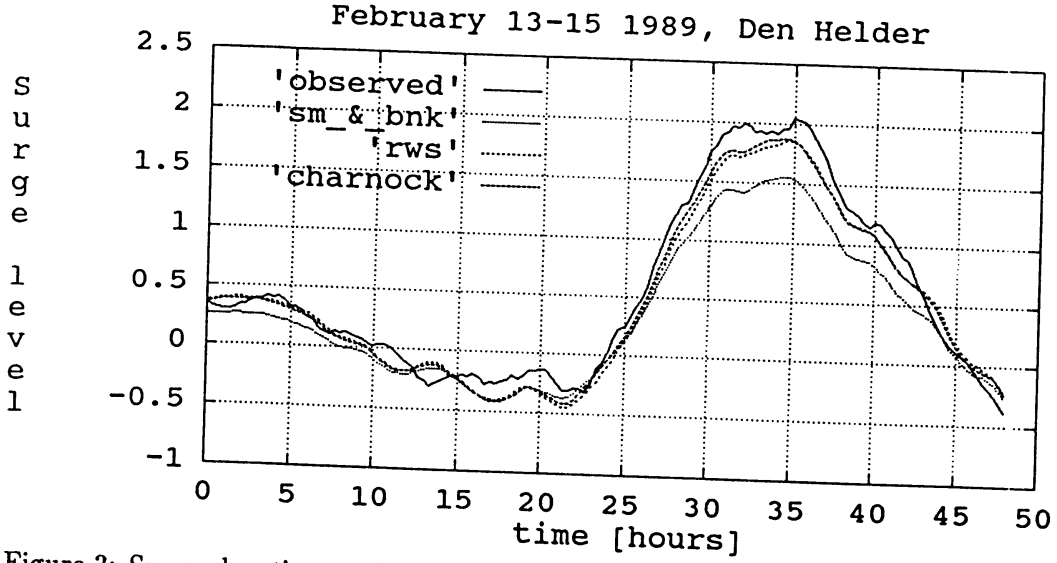

Figure 3: Surge elevations at Den Helder for the February 1989 storm for the three drag models. The continuous curve represents the observations, the dotted curve the Smith and Banke drag relation, the thin-dashed curve the RWS function, and the thick-dashed curve the Charnock function for β=0.031.

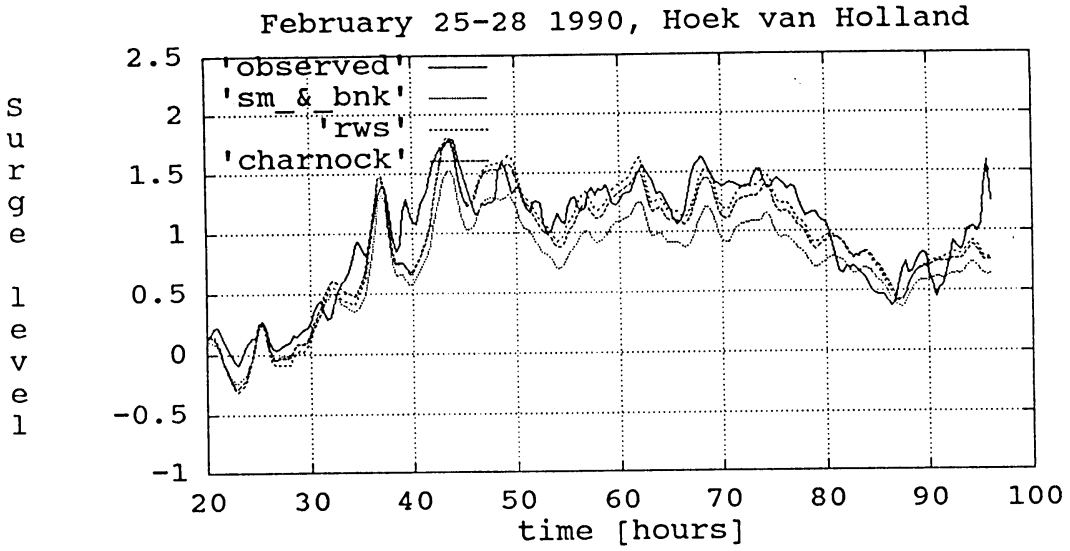

Figure 4: Surge elevations at Hoek van Holland for the February 1990 storm for the three drag models. The continuous curve represents the observations, the dotted curve the Smith and Banke drag relation, the thin-dashed curve the RWS function, and the thick-dashed curve the Charnock function for β=0.031.

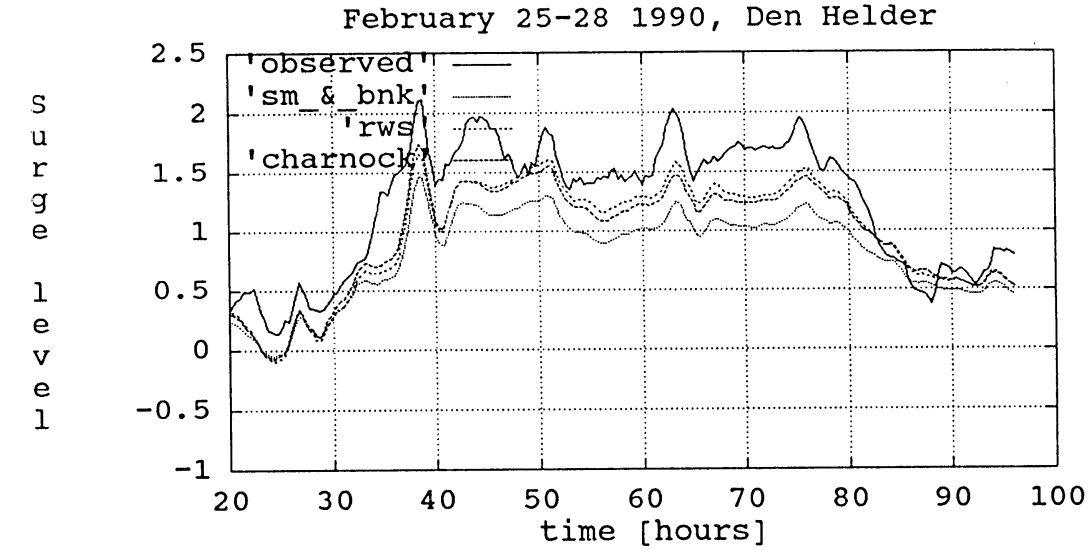

Figure 5: Surge elevations at Den Helder for the February 1990 storm for the three drag models. The continuous curve represents the observations, the dotted curve the Smith and Banke drag relation, the thin-dashed curve the RWS function, and the thick-dashed curve the Charnock function for β=0.031.

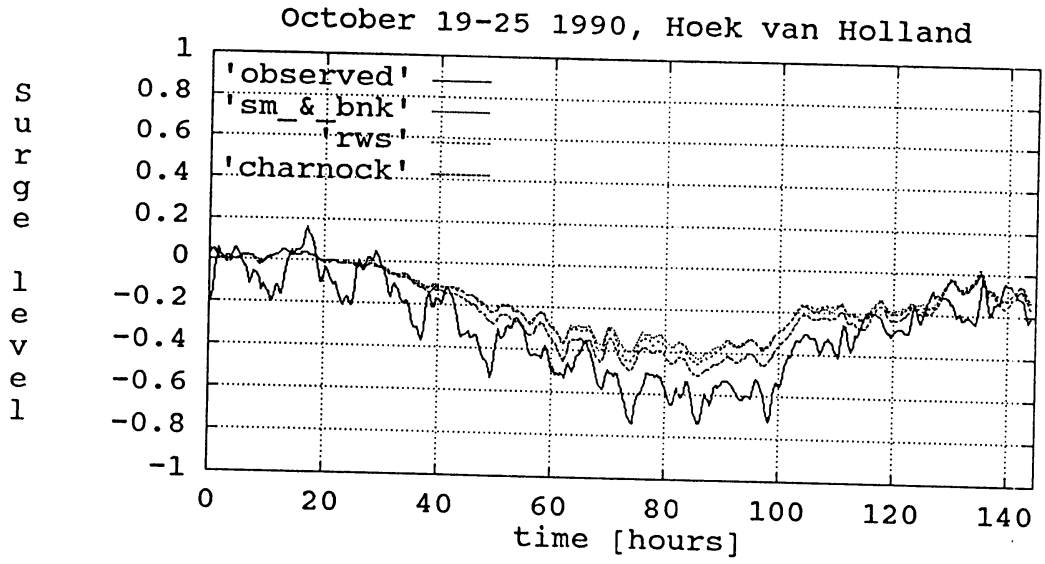

Figure 6: Surge elevations at Hoek van Holland for the October 1990 negative surge for the three drag models. The continuous curve represents the observations, the dotted curve the Smith and Banke drag relation, the thin-dashed curve the RWS function, and the thick-dashed curve the Charnock function for β=0.031.

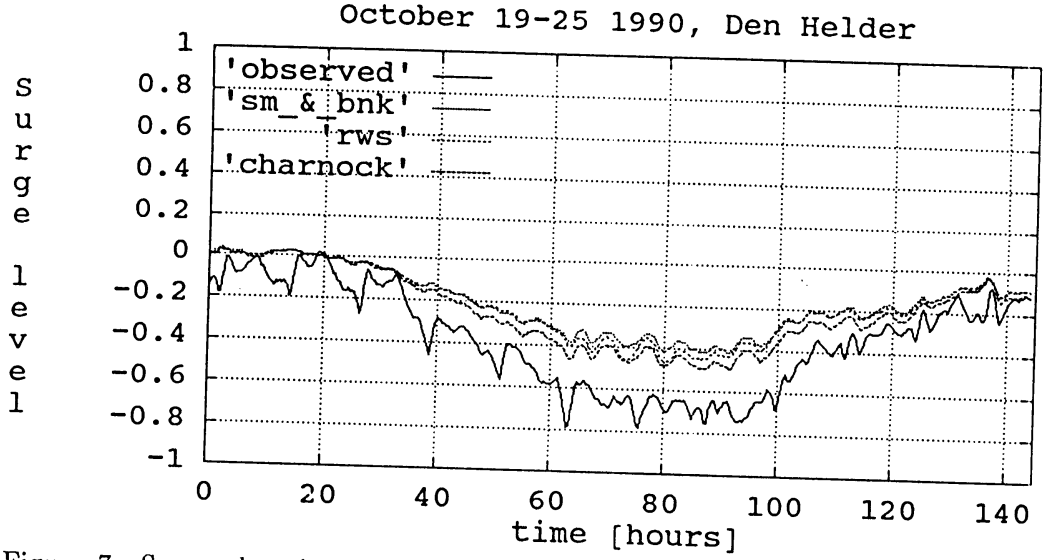

Figure 7: Surge elevations at Den Helder for the October 1990 negative surge for the three drag models. The continuous curve represents the observations, the dotted curve the Smith and Banke drag relation, the thin-dashed curve the RWS function, and the thick-dashed curve the Charnock function for β=0.031.

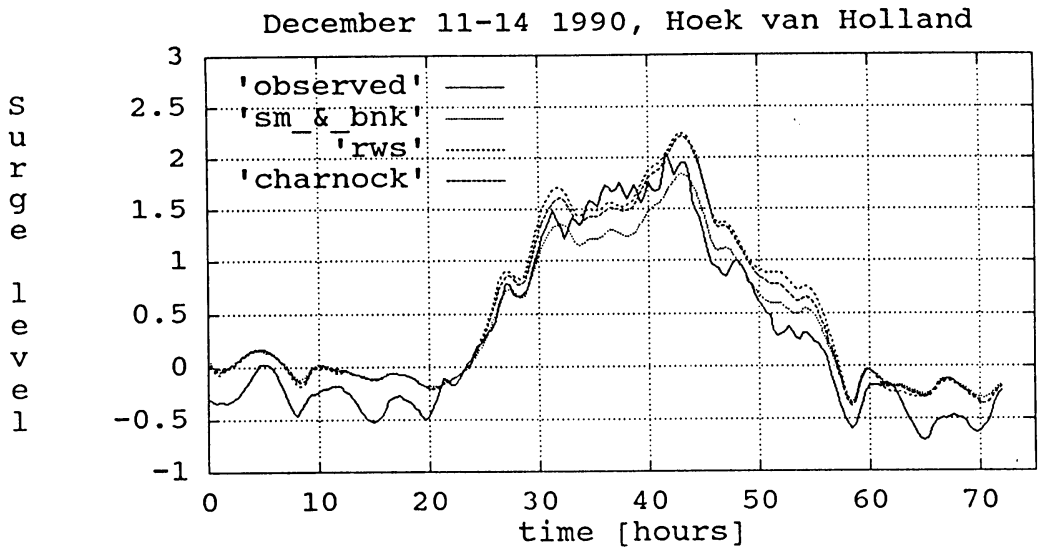

Figure 8: Surge elevations at Hoek van Holland for the December 1990 storm for the three drag models. The continuous curve represents the observations, the dotted curve the Smith and Banke drag relation, the thin-dashed curve the RWS function, and the thick-dashed curve the Charnock function for β=0.031.

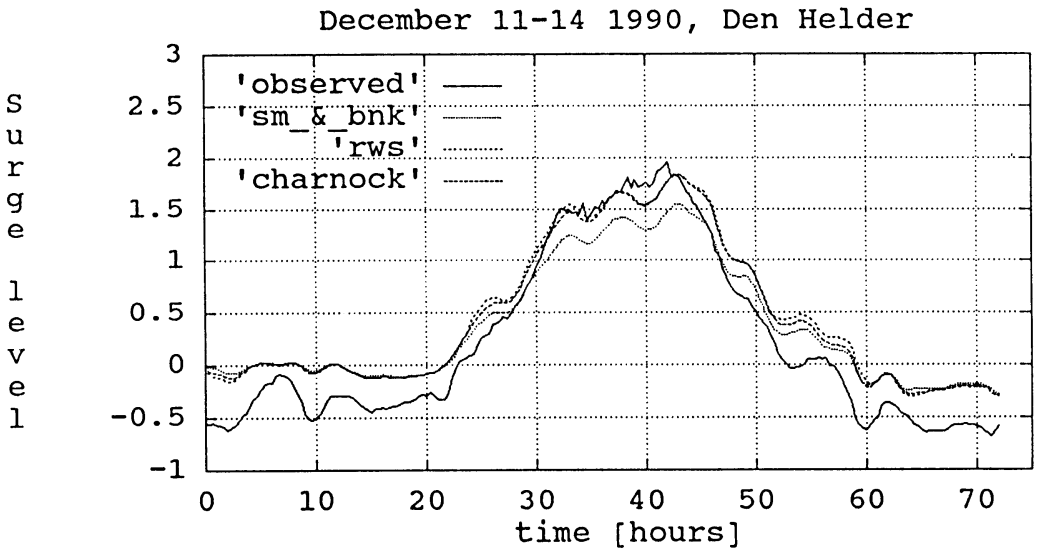

Figure 9: Surge elevations at Den Helder for the December 1990 storm for the three drag models. The continuous curve represents the observations, the dotted curve the Smith and Banke drag relation, the thin-dashed curve the RWS function, and the thick-dashed curve the Charnock function for β=0.031.

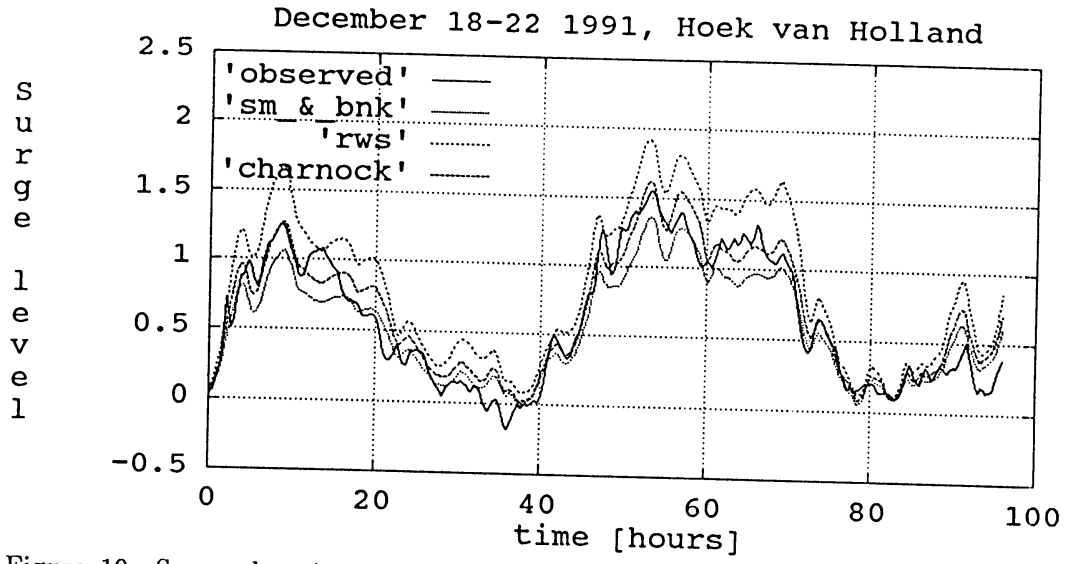

Figure 10: Surge elevations at Hoek van Holland for the December 1991 storm for the three drag models. The continuous curve represents the observations, the dotted curve the Smith and Banke drag relation, the thin-dashed curve the RWS function, and the thick-dashed curve the Charnock function for β=0.031.

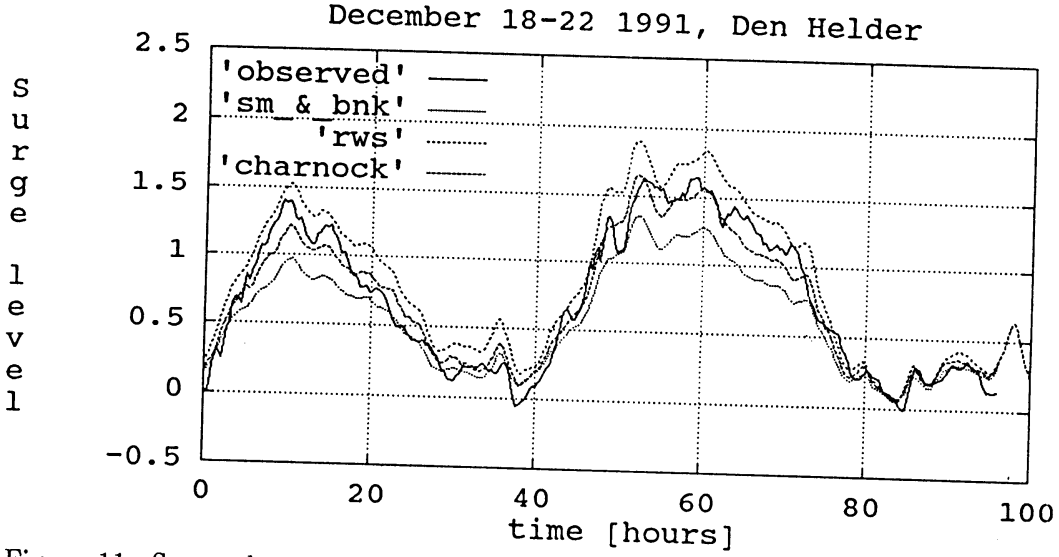

Figure 11: Surge elevations at Den Helder for the December 1991 storm for the three drag models. The continuous curve represents the observations, the dotted curve the Smith and Banke drag relation, the thin-dashed curve the RWS function, and the thick-dashed curve the Charnock function for β=0.031.

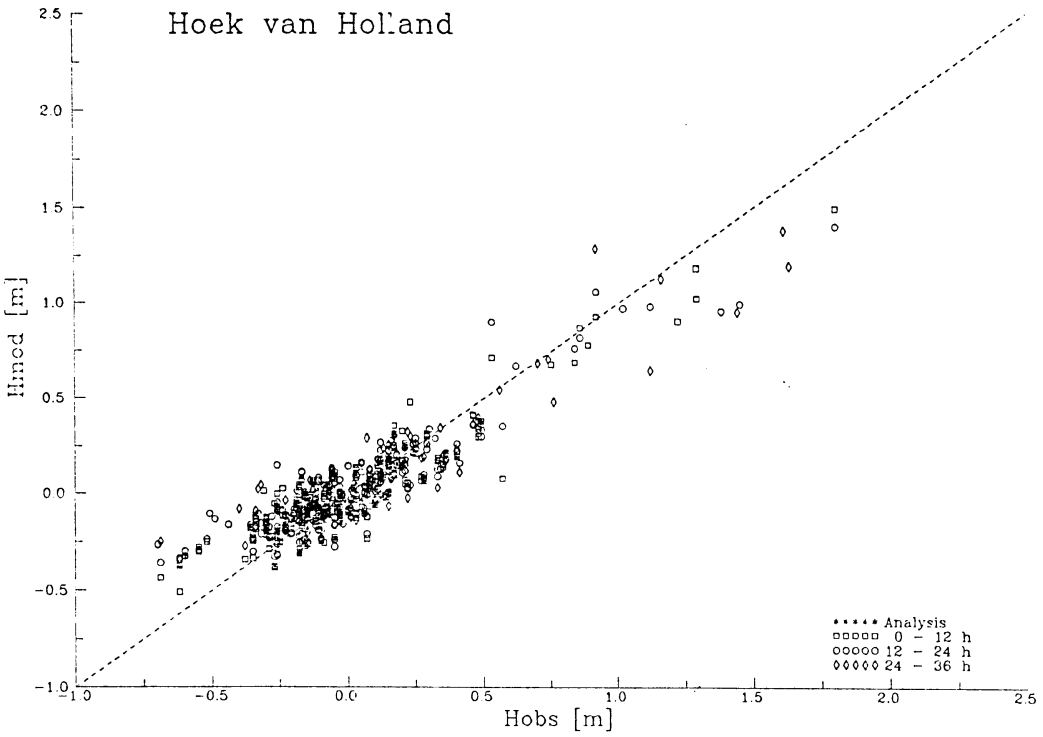

Figure 12: Scatter plot of calculated elevations H_{mod} versus observed values H_{obs} for Hoek van Holland, adopting the Smith and Banke drag coefficient.

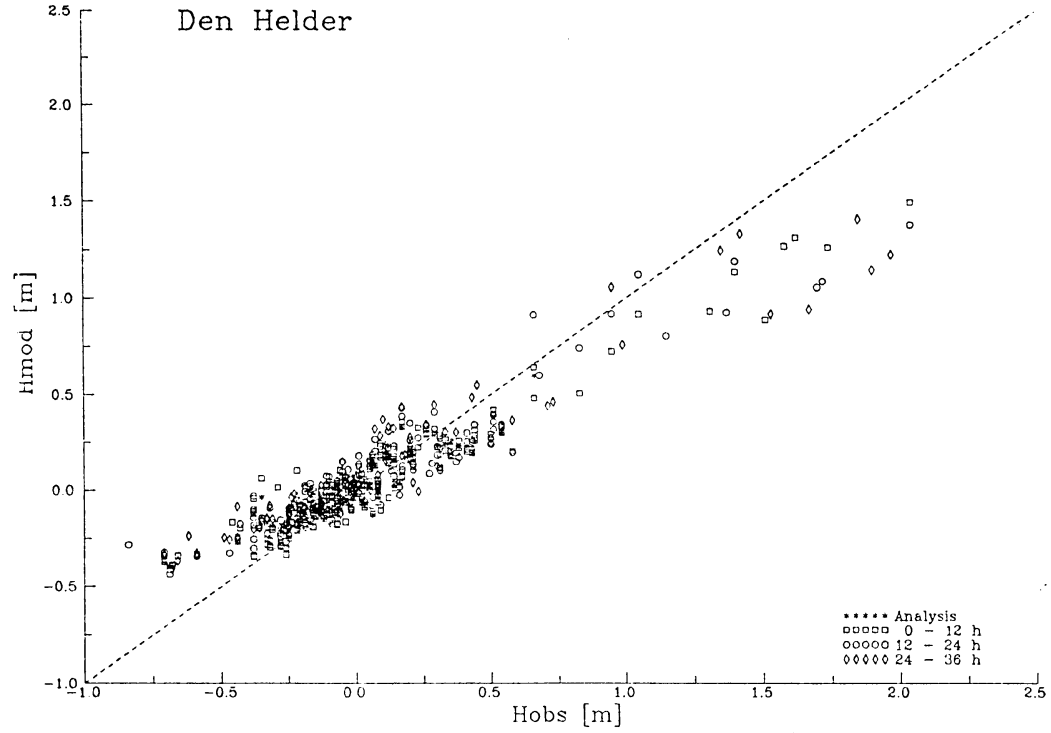

Figure 13: Scatter plot of calculated elevations H_{mod} versus observed values H_{obs} for Den Helder, adopting the Smith and Banke drag coefficient.

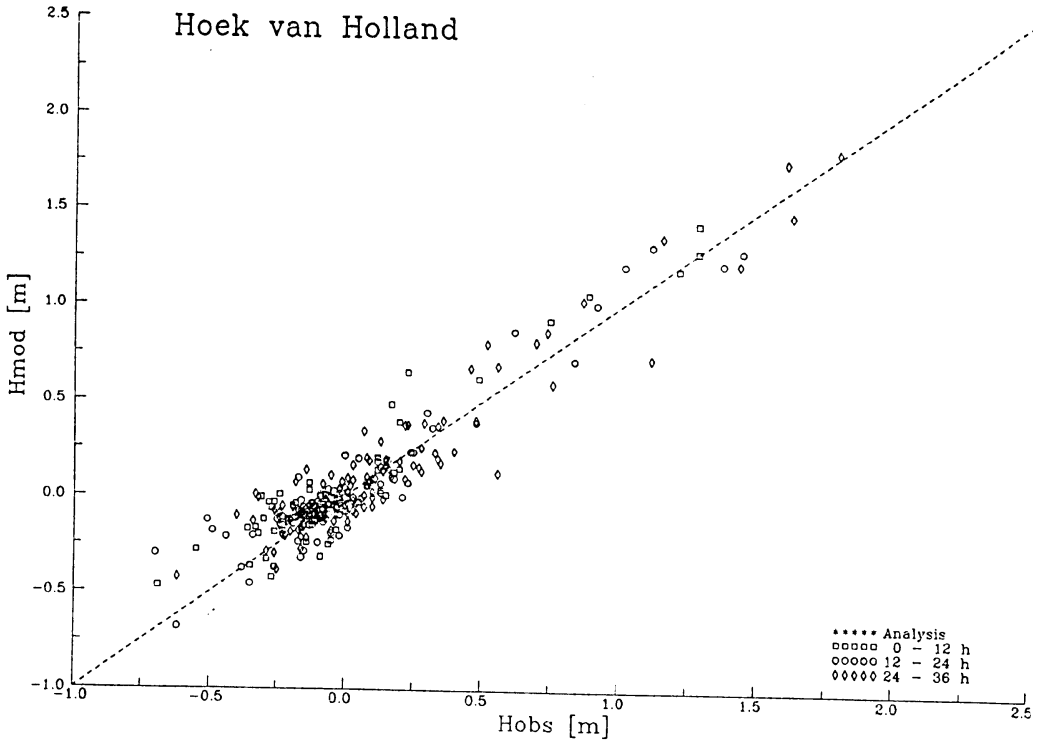

Figure 14: Scatter plot of calculated elevations H_{mod} versus observed values H_{obs} for Hoek van Holland, adopting the RWS drag coefficient.

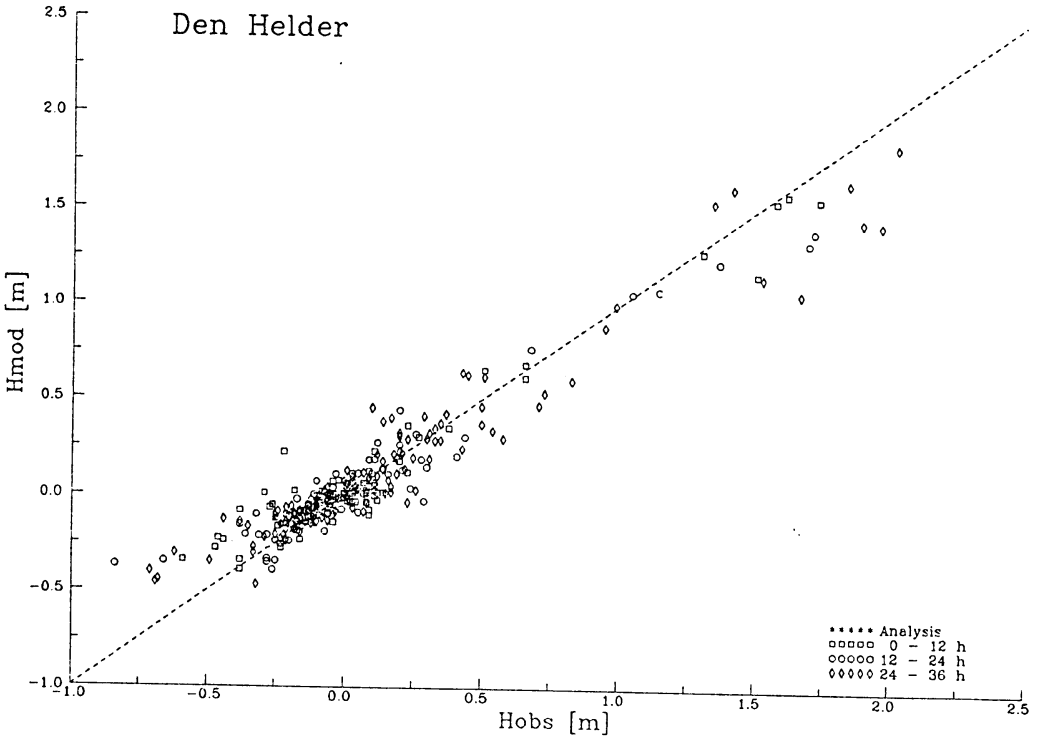

Figure 15: Scatter plot of calculated elevations H_{mod} versus observed values H_{obs} for Den Helder, adopting the RWS drag coefficient.

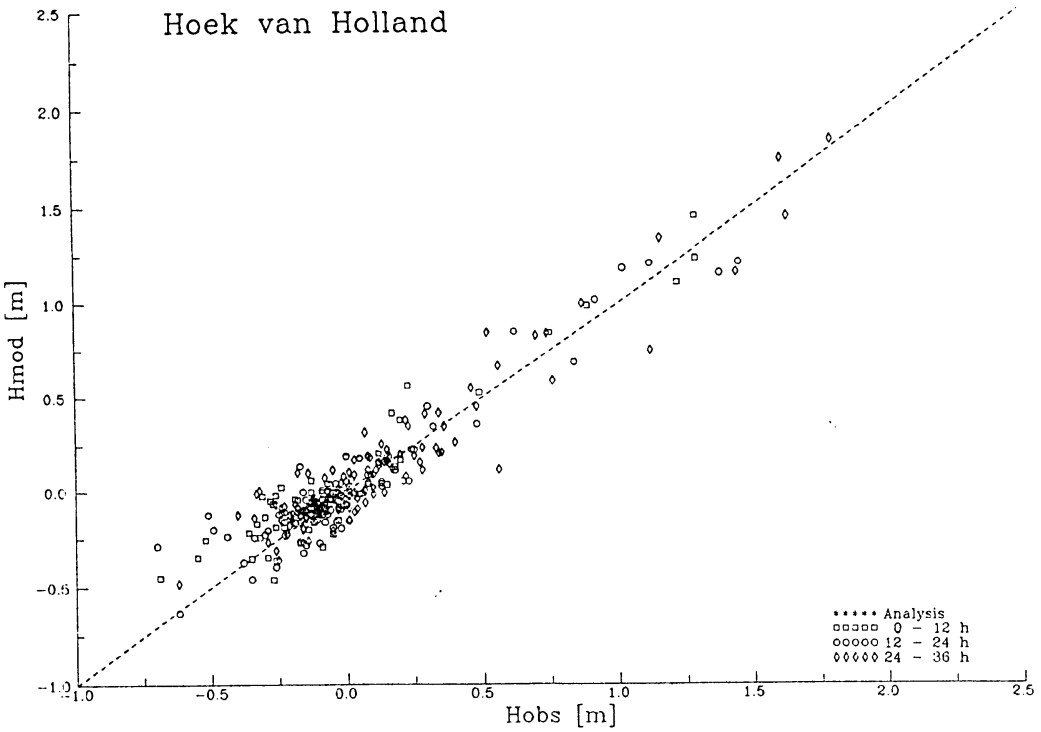

Figure 16: Scatter plot of calculated elevations H_{mod} versus observed values H_{obs} for Hoek van Holland, adopting the Charnock drag coefficient.

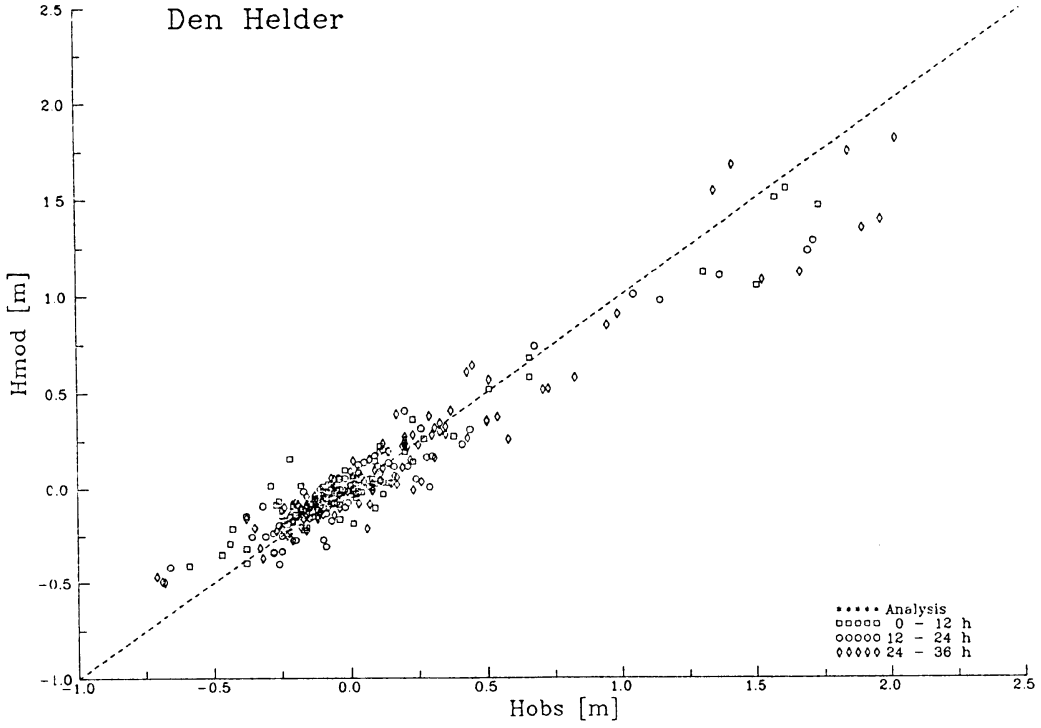

Figure 17: Scatter plot of calculated elevations H_{mod} versus observed values H_{obs} for Den Helder, adopting the Charnock drag coefficient.